Science Signaling
AAAS

www.sciencesignaling.org/cgi/content/full/2/55/ra4/DC1

Supplementary Materials for

EGFR Signals to mTOR Through PKC and Independently of Akt in Glioma

Qi-Wen Fan, Christine Cheng, Zachary A. Knight, Daphne Haas-Kogan, David Stokoe, C. David James, Frank McCormick, Kevan M. Shokat, William A. Weiss*

*To whom correspondence should be addressed. E-mail:weiss@cgl.ucsf.edu

Published 27 January 2009, *Sci. Signal.* **2**, ra4 (2009)
DOI: 10.1126/scisignal.2000014

The PDF file includes:

Fig. S1. Inhibition or knockdown of EGFR, Akt, PI3K, and mTOR in glioma; effects of serum.
Fig. S2. PMA interferes with the ability of erlotinib to decrease phosphorylation of rpS6 in *PTEN*^{wt} glioma cells regardless of *EGFR* status.
Fig. S3. Inhibition of PTEN leads to increased abundance of p-Akt in *PTEN*^{wt} LN229: *EGFR* cells.
Fig. S4. Knockdown of PKCα and PKCδ in LN229:*EGFR* glioma cells.
Fig. S5. Abundance of EGFR, p-PKCα, p-PKC (pan), p-rpS6, and p-Akt in normal brain and primary human glioblastoma tumors.
Fig. S6. A PKC inhibitor blocks proliferation in both *PTEN*^{wt} and *PTEN*^{mt} glioma cell lines.

Supplementary Materials for

EGFR signals to mTOR through PKC and independently of Akt in glioma

Qi-Wen Fan, Christine Cheng, Zachary A. Knight, Daphne Haas-Kogan,
David Stokoe, C. David James, Frank McCormick, Kevan M. Shokat,
and William A. Weiss*

*To whom correspondence should be addressed. E-mail:weiss@cgl.usf.edu

This PDF file includes:

Figure S1. Inhibition or knockdown of EGFR, Akt, PI3K and mTOR in glioma, effects of serum.

Figure S2. PMA interferes with the ability of erlotinib to decrease phosphorylation of pS6 in *PTEN*^{wt} glioma cells regardless of *EGFR* status.

Figure S3. Inhibition of Pten leads to increased abundance of p-Akt in *PTEN*^{wt} LN229*:EGFR* cells.

Figure S4. Knock-down of PKCα and PKCδ in LN229*:EGFR* glioma cells.

Figure S5. Abundance of EGFR, p-PKCα, p-PKC (pan), p-rpS6 and p-Akt in normal brain and primary human glioblastoma tumors.

Figure S6. A PKC inhibitor blocks proliferation in both *PTEN*^{wt} and *PTEN*^{mt} glioma cell lines.

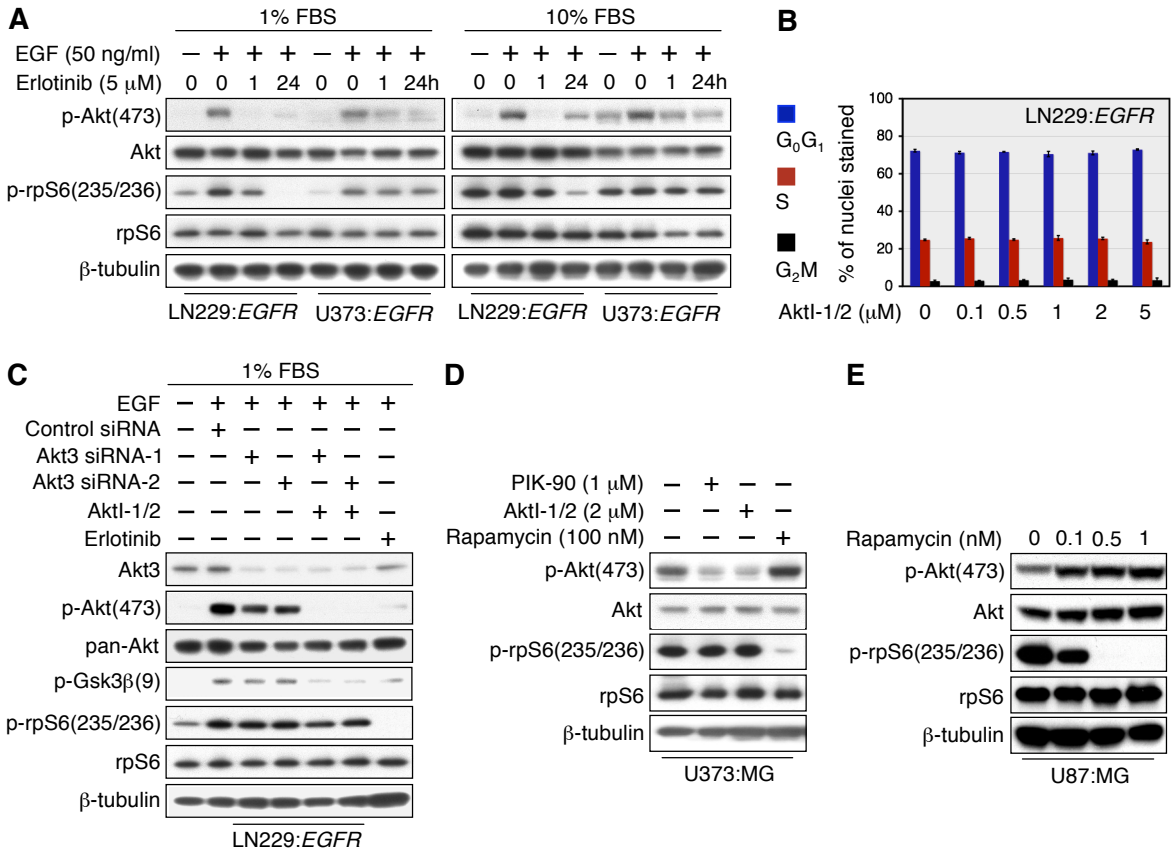

Fig S1. Inhibition or knockdown of EGFR, Akt, PI3K and mTOR in glioma; effects of serum. (**A**) Biochemical analysis of EGFR inhibition as a function of time and of serum concentration. Glioma cells in 1% or 10% FBS were treated with erlotinib (5 μM) for 1 or 24h as shown. EGF (50 ng/ml) was added 15 min prior to harvest for immunoblot. Although erlotinib blocked Akt in both *PTEN*^{wt} LN229:EGFR and in *PTEN*^{mt} U373:EGFR cells irrespective of serum concentration, the ability of erlotinib to affect the abundance of p-rpS6 was limited to *PTEN*^{wt} cells. (**B, C**). Small molecule inhibition (**B**) or siRNA knockdown of Akt isozymes (**C**) failed to affect proliferation or the mTOR target p-rpS6 in *PTEN*^{wt} LN229*:EGFR* cells. (**B**) LN229:*EGFR* cells (10% FBS) treated with AktI-1/2 at doses ranging from 0.1-5 μM showed no changes in cell cycle distribution. Percentage of cells in G_0G_1, S, and G_2M phase of the cell cycle is indicated. Data shown are means ± standard deviations for triplicate measurements. (**C**) Combined siRNA and small molecule inhibitor treatment in LN229*:EGFR* cells grown in 1% FBS for 48h led to undetectable p-Akt. Identical results were achieved using Akt3 siRNA-1 (Santa Cruz) and Akt3 siRNA-2 (Dharmacon). The abundance of p-rpS6 was either minimally affected or unaffected (note decreased levels of β-tubulin loading control in cells treated with both Akt3 siRNA-1 and AktI-1/2), whereas phosphorylation of the Akt target p-Gsk3β was decreased. Dosages were 2 μM (AktI-1/2) and 5 μM (erlotinib). (**D**) Small molecule inhibition of PI3K or Akt isozymes 1 and 2 failed to affect phosphorylation of the mTOR target rpS6 in *PTEN*^{mt} U373 MG cells. To extend results to *PTEN*^{mt} glioma, we analyzed both AktI-1/2 and the PI3K inhibitor PIK-90. Inhibition of PI3K, or Akt1 and Akt2 at doses effective against p-Akt again had no affect on p-rpS6. Rapamycin inhibited rpS6 phosphorylation, a result also observed in *PTEN*^{mt} U87:MG (**E**).

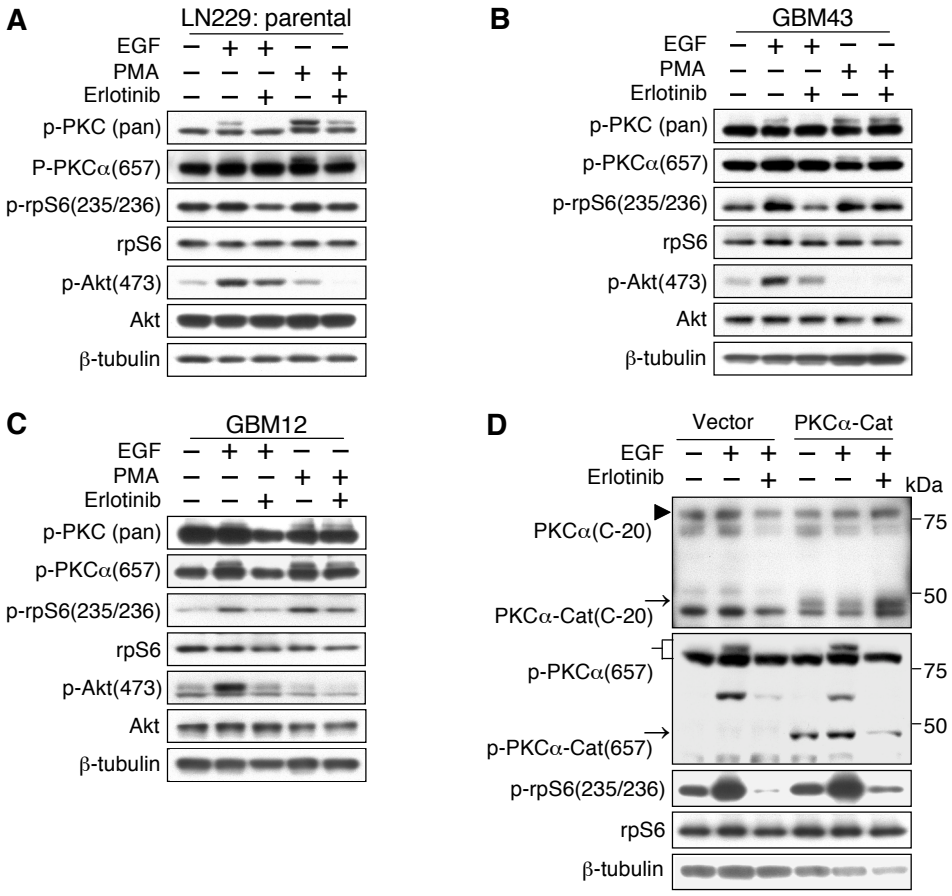

Fig S2. PMA interferes with the ability of erlotinib to decrease phosphorylation of p-rpS6 in *PTEN*^{wt} glioma cells regardless of *EGFR* status. To assess signaling between EGFR, PKCα, and mTOR in the absence or presence of *EGFR* amplification, we analyzed (**A**) LN229 parental cells, (**B**) GBM43, a primary glioma xenograft wild-type for both *PTEN* and *EGFR,* and (**C**) GBM12, a primary glioma xenograft wild-type for *PTEN* and amplified for *EGFR* . PMA (100 nM) elicited appearance of a slowly migrating p-PKCα band in all cell lines and primary xenografts. In EGF-treated cells, erlotinib (5 μM) transformed this apparent doublet to a single more rapidly migrating band. Erlotinib treatment also blocked increased p-rpS6 abundance in response to EGF. In PMA-treated cells, this doublet was still evident in the setting of erlotinib treatment and correlated with reduced activity of erlotinib against p-rpS6. (**D**) A dominant-active allele of PKCα [PKCα-Cat] blocks the biochemical activity of erlotinib (5 μM) against p-rpS6 in LN229*:EGFR* cells grown in 1% FBS. Immunoblot using antisera against C-terminus of PKCα shows levels of PKCα-Cat comparable to those observed for endogenous PKCα. Erlotinib (5 μM) blocked induction of p-rpS6 in control cells, but was less effective in cells transduced with PKCα-Cat. The effect seen is likely an underestimate, as PKC α-Cat cells treated with both EGF and erlotinib were underloaded on blot shown (note level of β-tubulin control).

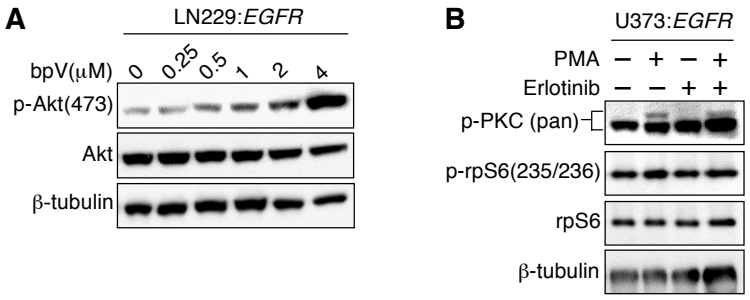

Fig S3. Inhibition of Pten leads to increased abundance of p-Akt in *PTEN*^{wt} LN229*:EGFR* cells. (**A**) *PTEN*^{wt} LN229*:EGFR* cells were treated with the Pten inhibitor bisperoxyvanadium for 24h at dosage indicated. Cells were lysed and immunoblotted as indicated. (**B**) *PTEN*^{mt} U373*:EGFR* cells were treated with erlotinib (5 μM) in the presence of PMA (100 nM) for 24h. Immunoblot shows appearance of a slowly migrating p-PKC protein in response to PMA, which was not affected by erlotinib.

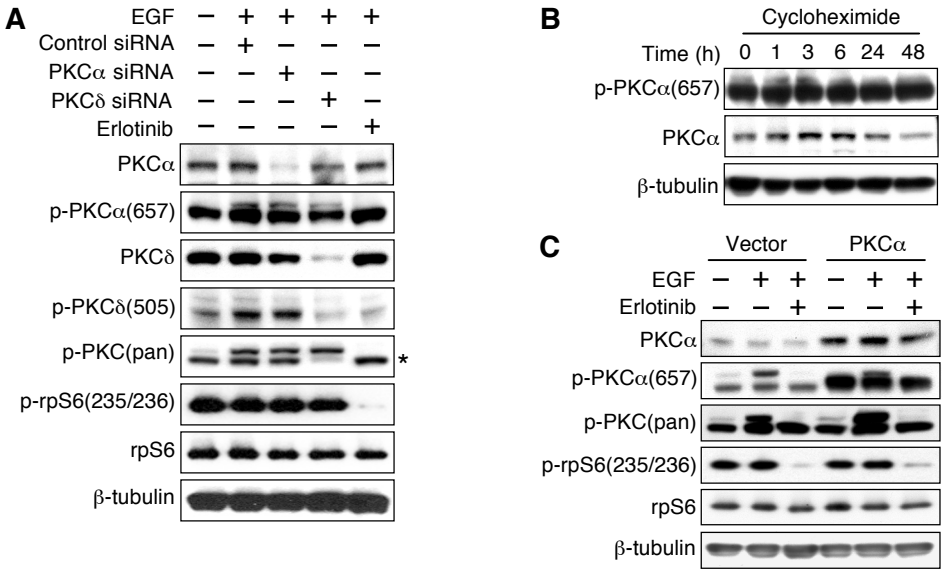

Fig S4. Knock-down of PKCα and PKCδ in LN229*:EGFR* glioma cells. (**A**) siRNAs directed against PKCα decreased the total abundance of PKCα without affecting the abundance of p-PKCα, suggesting that siRNA directed against PKCα could not be used to evaluate the role of p-PKCα. SiRNA against PKCδ blocked only the rapidly migrating phospho-PKCδ isoform, with no affect on the supershifted band, thereby excluding PKCδ as a critical intermediate between EGFR and mTOR. Erlotinib was added at 5 μM. (**B**) Pulse chase analysis in the presence of cycloheximide (an inhibitor of protein synthesis) demonstrates that p-PKCα has $t_{1/2}$~48h, explaining the high levels of p-PKCα observed after efficient knock-down of total PKC. Cycloheximide (25 μM) was added for times shown. Cultures were treated with EGF for 15 min prior to harvest. (**C**) LN229*:EGFR* cells transduced with PKCα showed increased abundance of PKCα and p-PKCα, validating the specificity of antibody reagents against these proteins. EGF dose was (50 ng/ml).

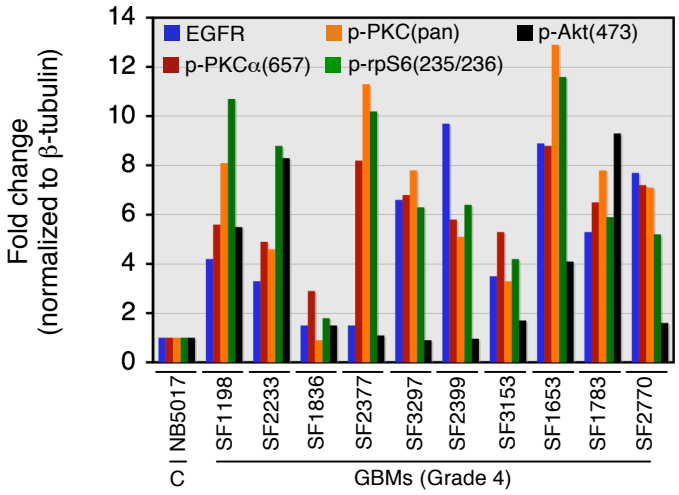

Fig S5. Abundance of EGFR, p-PKCα, p-PKC (pan), p-rpS6 and p-Akt in normal brain and primary human glioblastoma tumors (as compared to normal brain control and normalized to β-tubulin). Abundance of each protein in Fig 6 was quantitated using UMAX PowerLook Scanner and ImageJ software.

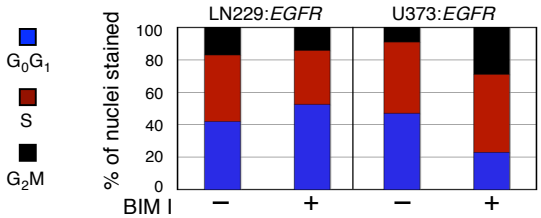

Fig S6. A PKC inhibitor blocks proliferation in both *PTEN*^{wt} and *PTEN*^{mt} glioma cell lines. *PTEN*^{wt} and *PTEN*^{mt} cell lines shown were treated with 5 μM of the pan-PKC inhibitor bisindolylmaleimide I (BIM I) for 24h. Flow cytometric analysis indicates percentage of cells in G_0G_1, S, and G_2M phases of the cell cycle. That BIM treatment led to arrest at G_1 in *PTEN*^{wt} LN229*:EGFR* and at G_2 in *PTEN*^{mt} U373*:EGFR* cells argues that the proliferative arrest induced by this agent results from on-target effects, rather than from non-selective toxicity.